

A statistical study on the geoeffectiveness of Earth-directed coronal mass ejections from March 1997 to December 2000

Y. M. Wang¹

National Astronomical Observatories of China, Beijing, China

P. Z. Ye and S. Wang

School of Earth and Space Sciences, University of Science and Technology of China, Anhui, China

G. P. Zhou² and J. X. Wang

National Astronomical Observatories of China, Beijing, China

Received 3 January 2002; revised 28 May 2002; accepted 30 May 2002; published 2 November 2002.

[1] We have identified 132 Earth-directed coronal mass ejections (CMEs) based on the observations of the Large Angle Spectroscopic Coronagraph (LASCO) and Extreme Ultraviolet Imaging Telescope (EIT) on board of Solar and Heliospheric Observatory (SOHO) from March 1997 to December 2000 and carried out a statistical study on their geoeffectiveness. The following results are obtained: (1) Only 45% of the total 132 Earth-directed halo CMEs caused geomagnetic storms with $K_p \geq 5$; (2) The initial sites of these geoeffective halo CMEs are rather symmetrically distributed in the heliographic latitude of the visible solar disc, while asymmetrical in longitude with the majority located in the west side of the central meridian; (3) The frontside halo CMEs accompanied with solar flares (identified from GOES-8 satellite observations) seem to be more geoeffective; (4) Only a weak correlation between the CME projected speed and the transit time is revealed. However, for the severe geomagnetic storms (with $K_p \geq 7$), a significant correlation at the confidence level of 99% is found. *INDEX TERMS:* 2788 Magnetospheric Physics: Storms and substorms; 7519 Solar Physics, Astrophysics, and Astronomy: Flares; 2111 Interplanetary Physics: Ejecta, driver gases, and magnetic clouds; 1739 History of Geophysics: Solar/planetary relationships; 7513 Solar Physics, Astrophysics, and Astronomy: Coronal mass ejections; *KEYWORDS:* CME, geomagnetic storm

Citation: Wang, Y. M., P. Z. Yee, S. Wang, G. P. Zhou, and J. Wang, A statistical study on the geoeffectiveness of Earth-directed coronal mass ejections from March 1997 to December 2000, *J. Geophys. Res.*, 107(A11), 1340, doi:10.1029/2002JA009244, 2002.

1. Introduction

[2] Coronal mass ejections (CMEs), the large-scale eruptions of plasma and magnetic fields from the Sun [Hundhausen, 1993], are now believed to be the main source of the strong interplanetary disturbances (including shocks) that cause many nonrecurrent geomagnetic storms [Sheeley *et al.*, 1985; Gosling *et al.*, 1991] and may also play a role in the largest recurrent storms as well [Crooker and Cliver, 1994; Crooker and McAllister, 1997]. However, it is not very clear yet what kinds of CMEs can result in large geomagnetic storms. In other words, it is still difficult to predict geomagnetic storms on the basis of the CME observations. Since CMEs can be approximated as spherically symmetric structures, halo CMEs are thought directing toward or away from the Earth [Howard *et al.*, 1982]. Those frontside halo CMEs,

or the Earth-directed CMEs which initiate from the visible solar disc, are more likely to affect the geomagnetosphere than others. However, not all of the frontside halo CMEs can drive moderate to intense geomagnetic storms. A prediction based only on the occurrence of frontside halo CMEs often has a high “false alarm” rate [St. Cyr *et al.*, 2000].

[3] The connection between Earth-directed CMEs and geomagnetic storms has been discussed by Brueckner *et al.* [1998]. They discovered that all but two geomagnetic storms with $K_p \geq 6$ during the period from March 1996 through June 1997 could be associated with CMEs. The average travel time between the solar explosion and the onset of the maximum K_p value was ~ 80 hours. However, there were only eight events with $K_p \geq 6$ during their reported period. Webb *et al.* [2000] analyzed the relationship of halo CMEs, magnetic clouds, and geomagnetic storms. They found that all six halo CMEs that were likely Earth-directed were associated with shocks, magnetic clouds, and moderate geomagnetic storms at Earth 3–5 days later, during the solar minimum period from December 1996 to June 1997. These geomagnetic storms had peak K_p levels of 4 to 7 and peak Dst levels of -41 to -115 , respectively.

¹Also at School of Earth and Space Sciences, University of Science and Technology of China, Beijing, China.

²Also at Anhui University, Anhui, China.

On the basis of this sample the authors also discussed in detail the CME characteristics, their signatures near the solar surface, and their usefulness as predictors of space weather at the Earth. *Cane et al.* [2000] further studied the relationship of CMEs, ejecta, and geomagnetic storms during 1996–1999. They found that only about half of frontside halo CMEs encountered the Earth and their associated solar events typically occurred from east 40° to west 40° in longitude.

[4] To predict the arrival of CMEs to 1 AU, the relationship between the CMEs speed and the ejecta travelling time in interplanetary space has been studied by some authors [e.g. *Gopalswamy et al.*, 2000, 2001a; *Cane et al.*, 2000]. *Gopalswamy et al.* [2000, 2001a] proposed an empirical model to predict ejecta arrival times on the basis of observations from the Solar and Heliospheric Observatory (SOHO), Wind, P78-1/PVO-Helios, and so on. In these studies they considered the acceleration of CMEs and the effects of projection which were beneficial to the forecast of geomagnetic storms.

[5] Since there were few high-cadence observations by the Extreme Ultraviolet Imaging Telescope (EIT) on board of SOHO before March 1997 because of telemetry restrictions [*Subramanian and Dere*, 2001], our data were selected from March 1997 to December 2000. In this paper we identified the entire frontside halo CMEs during this period and statistically analyzed the characteristics of geoeffective halo CMEs by correlating the frontside halo CMEs with geomagnetic storms directly. Then we derived the relationship between the CME projected speed and the “transit time.” The term “transit time” is defined as the interval from the first appearance of a CME in the Large Angle Spectroscopic Coronagraph (LASCO) C2 to the time of the maximum Kp value in a geomagnetic storm. It is similar to the convention of *Brueckner et al.* [1998] but unlike that used in other works [e.g. *Gopalswamy et al.*, 2000, 2001a; *Cane et al.*, 2000], in which the “transit time” denotes the travel time of CME/ejecta from the Sun to the Earth. Section 2 is devoted to the data and method in identifying the frontside halo CMEs and geoeffective CMEs. In section 3 we present our main statistical results. In section 4 we give a brief summary and discuss the problem with the prediction of geomagnetic storms.

2. Data and Method

2.1. Identification of Frontside Halo CMEs

[6] *Webb et al.* [2000] and *Cane et al.* [2000] used 140° span angle as a threshold apparent size to define halo CMEs. *St. Cyr et al.* [2000] used 120° span angle as a threshold to study the halo CMEs. Here, we followed the convention of *Hudson et al.* [1998] by using the term “halo CME” when the apparent size of a CME is greater than 130°. On the basis of the “LASCO CME catalog” compiled by Seiji Yashiro and Grzegorz Michalek under the guidance of Nat Gopalswamy (see http://cdaw.gsfc.nasa.gov/CME_list/index.html), we selected out the 350 halo CMEs from March 1997 to December 2000. During this period, there are several data gaps: 98/06/25–98/10/20, 98/11/13–98/11/22, 98/12/21–99/02/04, 99/02/15–99/02/20, and so on. For these gaps we simply cut them out

from this period and eliminated the corresponding geomagnetic data when discussing the geomagnetic storms. By scrutinizing the LASCO C2/C3 images and EIT images, we identified 132 definitive frontside CMEs from all of 350 halo CMEs. Their initial sites, i.e., the source regions where the CMEs first initiated, were located on the solar disk by carefully viewing EIT movies. The details in identifying the CME source region are illustrated by the following example.

[7] A halo CME, erupting on 10 June 2000, showed first appearance in LASCO/C2 at 1708 UT. The time T (≈ 1640 UT) of its initiation could be deduced by using the linear fit speed listed in the CME catalog. To justify whether the CME occurred on the frontside or backside, EIT running difference movie was studied carefully. The CME signatures in the lower corona, e.g., dimming, EIT wave and/or filament eruption, were always the necessary criteria to identify corresponding CME in EIT running difference movie. With these criteria we considered that any solar event, which satisfied the following conditions, might be associated with a given CME: (1) its location on the solar disk was consistent with the ejection direction of the corresponding CME seen in LASCO, (2) it occurred within the time window $T \pm 0.5$ hours, where T is the time of the CME initiation obtained by linear extrapolation as mentioned above, and (3) there was no sign on the background in EIT 195Å to indicate the CME possibly occurring on the backside. Hence for the CME, which could be found the associated frontside solar events, we considered it frontside or Earth-directed, and its initial location could be determined with some confidence. Using the EIT images with overlaid grid, as shown in Figure 1, we could estimate the coordinate of the initial site easily. From Figure 1 an evident eruption accompanied with an obviously large dimming began at 1635 UT, which was very close to the estimate time T . Also, the estimated initial location (N20W40) on solar disk was consistent with the direction of the CME in LASCO. Thus we concluded that this CME was frontside halo CME, and its initial site was at N20W40.

[8] Although CMEs were a large-scale phenomenon, they were always first triggered at a localized site, which we call the initial site or initial location here. In our statistics, almost all of these 132 frontside halo CMEs erupted in large regions, but the initial locations could always be limited in relatively small regions with the overlaid grids. An error of approximate 10° could be estimated while we were locating the CME initial site. Undoubtedly, the more distant away from the center meridian the initial location was, the larger was error in positioning the CME initiation. Moreover, for some of these CMEs, the initial locations were not the same as the sites of associated flares by the reason that the flares did not always erupt there where CMEs were first triggered.

[9] In the process of identification we found that not all of the observations were good enough to distinguish the frontside and backside CMEs. The rather poor cadence and the limited sensitivity of some EIT and LASCO data might bring some ambiguity in selecting Earth-directed events. For the safety of the conclusion we eliminated all the events whose identifications were ambiguous, and only left the definitively identified 132 halo CMEs in our study sample of frontside CMEs.

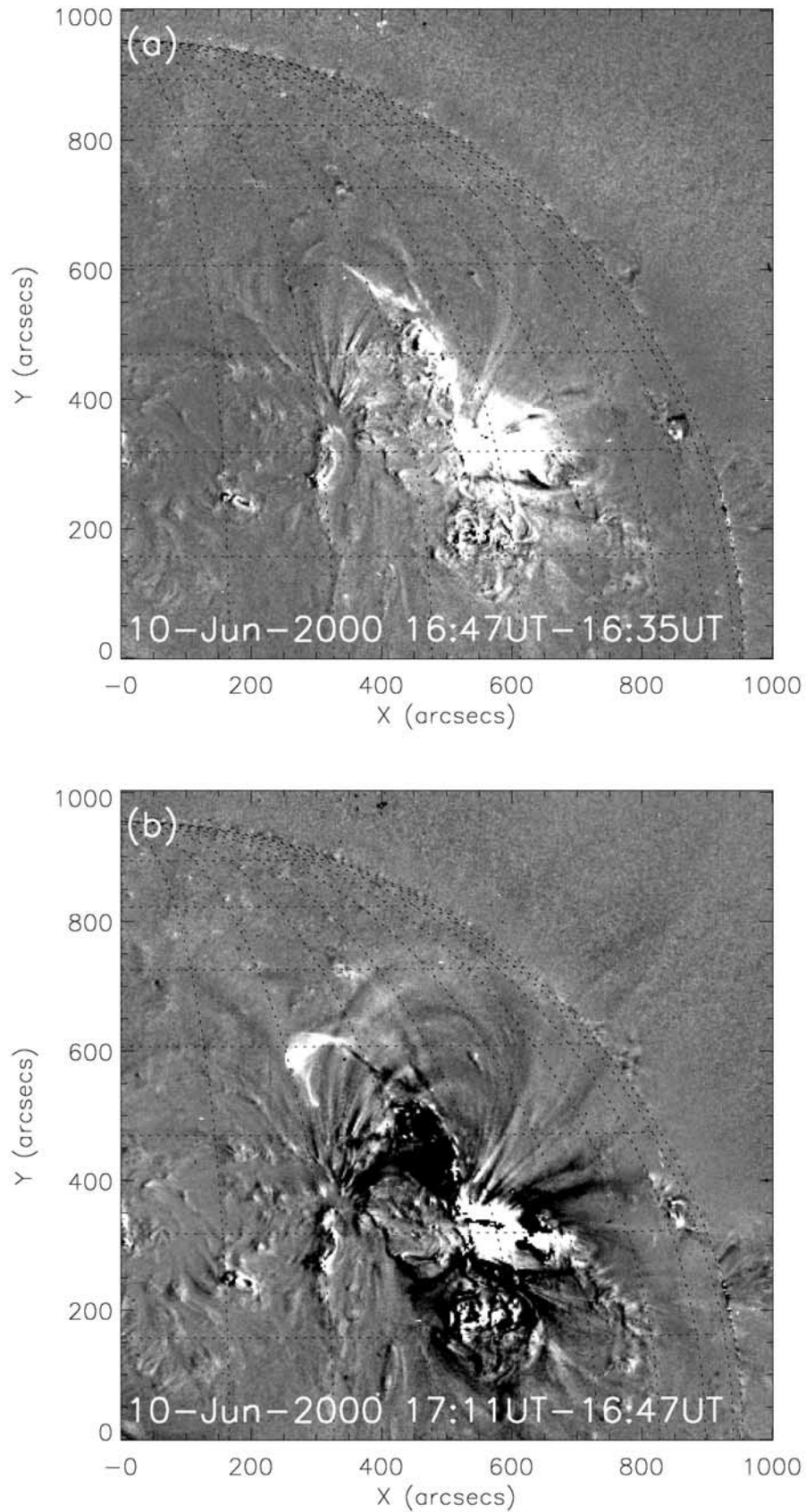


Figure 1. Running-difference images obtained by EIT 195Å on 10 June 2000. A large-scale EUV dimming began at ~1635 UT and the initial site of this event was located at approximately N20W40.

2.2. Frontside Halo CMEs Associated With Geomagnetic Storms

[10] To study the relationship between frontside halo CMEs and geomagnetic storms, we identified all the solar-terrestrial events associated with planetary index $K_p \geq 5$ during this period by considering many parameters, including solar wind speed, interplanetary magnetic field, proton temperature, and density observations from Wind spacecraft [e.g., *Cliver et al.*, 1990; *Richardson and Cane*, 1995; *McAllister and Crooker*, 1997; *Lindsay et al.*, 1999; *Webb et al.*, 1998, 2000; *Gopalswamy et al.*, 2000, 2001a, 2001b]. The planetary index K_p was obtained from World Data Center for Geomagnetism (via the web site <http://swdcd.db.kugi.kyoto-u.ac.jp/kp/index.html>). To be consistent with the period of CME data, we also dropped those periods during which there were no observations from SOHO.

[11] To identify the solar-terrestrial events, we first investigated whether there were $K_p \geq 5$ geomagnetic storms within several days after the frontside halo CMEs explosion. If there was none, the given frontside halo CME was considered to be definitely nongeoeffectiveness. Otherwise, if there were one storm following the CME we would examine further the characteristics of the interplanetary magnetic field (IMF) before the beginning of the geomagnetic storm in solar magnetospheric coordinate system (GSM). Generally, several hours before the K_p maximum, there was strong long-duration southward IMF, usually called Bs event, which plays a crucial role in determining the amount of solar wind energy to be transferred to the magnetosphere [e.g. *Arnoldy*, 1971; *Akasofu*, 1981; *Gonzalez and Tsurutani*, 1987]. The strong southward IMF might be in the magnetic cloud (MC) or might not be in the MC but in the region ahead of the MC where the shock compresses and deflects ambient solar wind [*Tsurutani et al.*, 1988]. An MC was identified by the following necessary observational features: (1) enhanced magnetic field strength, (2) a large and smooth rotation of the magnetic field direction and (3) low proton temperature [*Burlaga et al.*, 1981; *Osherovich and Burlaga*, 1997]. To find out the corresponding CME by a known strong southward IMF, we followed *Lindsay et al.* [1999] using MC speed or maximum solar wind flow speed (if the interplanetary ejecta was not MC) to estimate the time of potential CME initiation and select the most likely CME from the list. Then we correlated the CMEs with the geomagnetic storms directly and obtained the interval from occurrence of CME to the K_p maximum. For the safety of the result those ambiguous events without MC and shock were excluded. Moreover, some moderate storms were verified to be caused not by CMEs but by Earth passing through the heliospheric current sheet and related corotation interaction regions (CIRs) [e.g. *McAllister and Crooker*, 1997; *Webb et al.*, 2001], so they were also removed out from our statistics.

[12] For instance, Figure 2 shows a typical MC. Shock arrived at 1830 UT on 11 August 2000 and the MC began at approximately 0530 UT on the next day. On the same day (12 August), a severe geomagnetic storm ($K_p = 8$ -) occurred and K_p value reached the maximum at 1100 UT, marked by a triangle in the second panel of Figure 2. It took place ~ 5 hours after the beginning of strong southward IMF. The MC speed was about 680 km/s and we could obtain the estimate time, which is the same as the reference time T mentioned in

section 2.1, of the corresponding CME's eruption (~ 61 hours ago, i.e., at 1630 UT on 9 August) by supposing approximate constant speed for the CME in the interplanetary space. Since it was not known whether deceleration or acceleration has occurred in the actual travel, we applied a window of 12 hours centered on the estimate time of the CME's eruption (also refer to *Lindsay et al.* [1999]) to search the CMEs. In this time window we found that the frontside halo CME, first appeared at 1630 UT in LASCO/C2, satisfied the condition. Thus we deduced the transit time of this solar-terrestrial event is ~ 66.5 hours (including the interval from the arrival of MC to the K_p maximum). Sometimes there were several candidates in the time window so that it was more difficult to select the correct one. If the source regions of these candidates located at different sites, we assumed that they did not interact each other. For this case we utilized the curve about maximum in situ solar wind speed of disturbances versus the associated shock transit speed [*Cliver et al.*, 1990] to select the CME which fit the curve best. This method could not be used when there was no associated shock. Fortunately, we did not encounter such an embarrassing situation. On the other hand, if these candidates extended from the same source region and had similar behavior, we thought that this event had multiple sources, so we related the corresponding K_p storm with the first CME.

[13] Using this identification method, we found that 59 of the 132 frontside halo CMEs led to 51 $K_p \geq 5$ storms. Only 59/132 (45%) frontside halo CMEs could result in moderate to severe geomagnetic storms. This confirms the conclusion derived by *Cane et al.* [2000]. It is worth to note that the number of geoeffective halo CMEs is greater than that of the storms with $K_p \geq 5$ owing to the fact that in some cases several CMEs caused only one storm. For instance, the three CMEs, which appeared on 24 November 2000, caused one geomagnetic storm on 27 November. Those CMEs had erupted from the same active region, had similar extended EUV dimming, and had similar appearance in the coronagraph field of view [*Zhang and Wang*, 2002].

3. Results

3.1. Characteristics of Initial Location of the Geoeffective Halo CMEs

[14] Figure 3a shows the initial location distributions of these geoeffective halo CMEs on the meshed solar disc. From this figure the event initial locations appeared symmetrical about the equator. The majority of these CMEs (81%) occurred within latitude $\pm(10^\circ-30^\circ)$. Only two events were out of the latitude $\pm 40^\circ$. However, these were not the specific characteristics of geoeffective halo CMEs. As further demonstration, Figure 3b shows the distribution of all the frontside halo CMEs. They also were symmetrical about equator and mainly ($\sim 78\%$) located within latitude $\pm(10^\circ-30^\circ)$. Like geoeffective ones, there were only 8% frontside halo CMEs erupting outside of the latitude $\pm 40^\circ$.

[15] In Figure 3a we noticed that most of these events occurred in the vicinity of center meridian. Almost 83% of events took place within $\pm 30^\circ$ of center meridian. However, we could claim for an asymmetry in the center meridian distance (CMD) distribution. On the west, a geoeffective halo CME could be expected even at $\sim 70^\circ$. However, there was no one geoeffective halo CME outside of east 40° . The

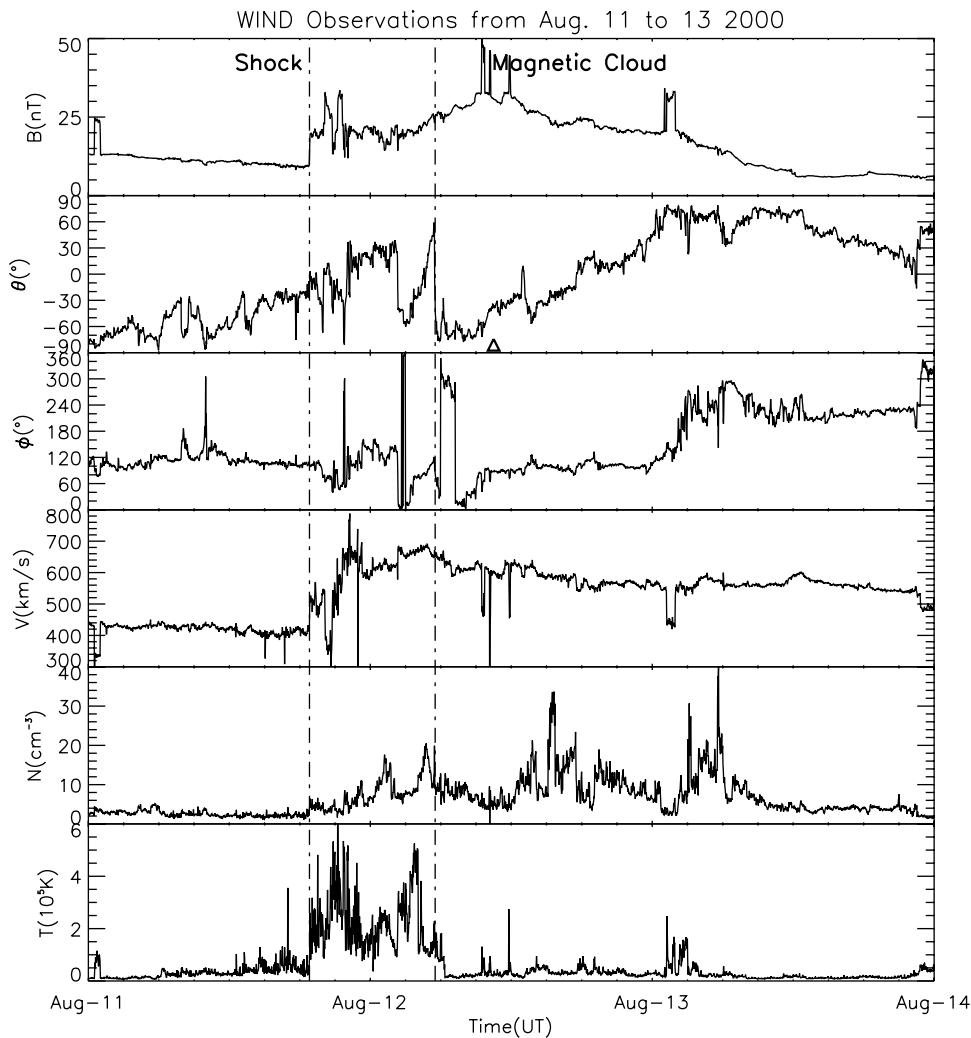


Figure 2. Observations of solar wind plasma and IMF by Wind spacecraft from 11–13 August 2000. From top to bottom are plotted magnetic field strength B , the elevation θ and azimuthal ϕ angles of the field direction, solar wind speed V , proton density N , and the moment proton temperature T . Vertical lines denote, from left to right, the times of the shock and the leading edge of the magnetic cloud. The triangle plotted in the second panel marks the arrival of Kp maximum.

number of geoeffective halo CMEs occurred on the west is $\sim 57\%$ greater than that on the east.

3.2. Solar Flares Associated With Halo CMEs

[16] By using the observations of X-ray flares from the GOES-8 satellite, we found that $\sim 70\%$ frontside halo CMEs were associated with flares with importance greater than C (as listed in Table 1). For geoeffective ones the percentage increased to 85%. This period from March 1997 to December 2000 was just the ascending phase of solar cycle 23 [Schatten *et al.*, 1996]. Coincidentally, the percent listed in Table 1 was on the increase year by year. The “increment” entry denotes the occurrence percent of geoeffective halo CMEs associated with solar flares was always larger than that of frontside ones generally. Especially in 2000 when the solar maximum was approaching, almost all of the geoeffective halo CMEs were related with flares (greater than C) except for one. Although there are some data gaps, we considered that the defect would not cause significant distortion on this result in the statistical study. The result seems

to imply that a CME is more likely to affect the geomagnetosphere if it was accompanied by some flare.

3.3. Relationship Between Projected Speeds of Geoeffective Halo CMEs and Transit Times

[17] As defined in section 1, here the “transit time” denotes the interval from CME first appearance in C2 to the time of the Kp maximum. For the situation that several CMEs caused one geomagnetic storm we dealt with them as one solar-terrestrial event and estimated the transit time from the first appearance of the first CME to the Kp maximum. It should be noted that the transit time used here was not the same as the other transit times which have been used in different authors’ works [e.g., Gopalswamy *et al.*, 2000, 2001a; Cane *et al.*, 2000]. Cane *et al.* [2000] based on cosmic ray depression to estimate the “transit time” by using the 1 AU arrival of ejecta. Gopalswamy *et al.* [2000, 2001a] used the magnetic signatures to obtain the arrival of ICME. Thus it is obvious that our “transit time” is larger than theirs if the geomagnetic storm is caused by southward

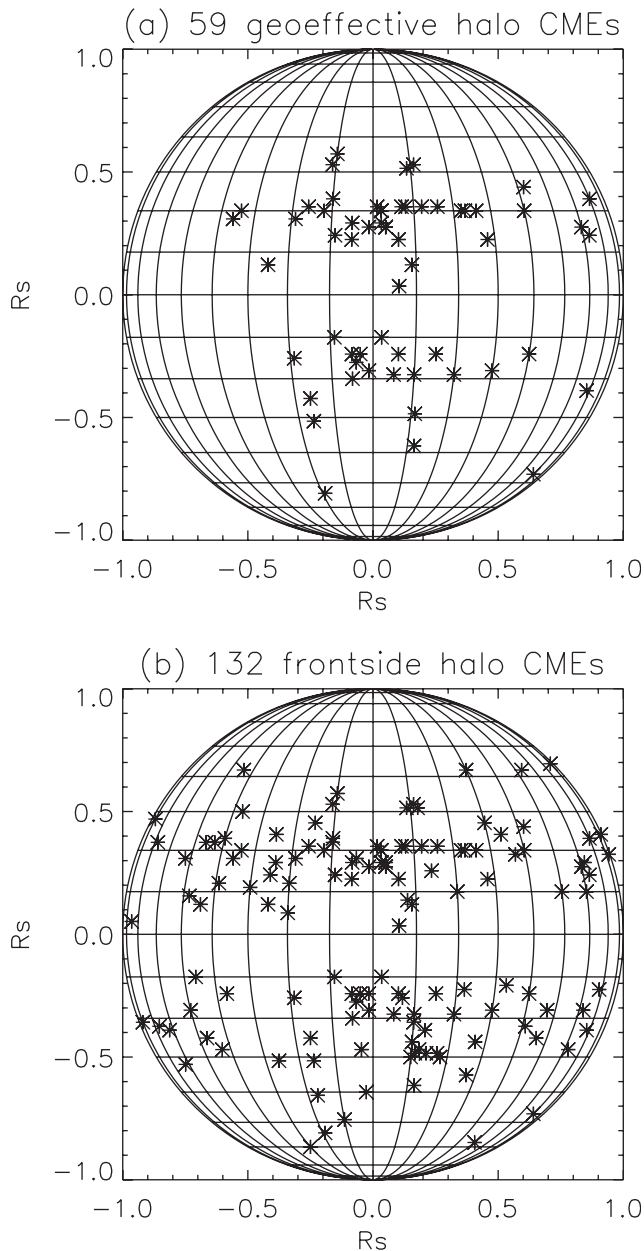


Figure 3. Initial location distribution of (a) geoeffective halo CMEs and (b) frontside halo CMEs on the solar disk. An asymmetrical characteristic of geoeffective halo CMEs in the longitude distribution is obvious in top panel.

field in MC. If geomagnetic storm is caused by shock sheath, our “transit time” is usually smaller than or the same as theirs. The first appearances and the projected speeds of these CMEs were also gained mostly from the CME catalog. For a few events we went back to the original data for a more accurate estimation. Allowing the errors by rather poor cadence of the LASCO and EIT data, we used linear fit speed.

[18] Figure 4 shows the transit time versus the CME projected speed, for events with $Kp \geq 5$ and $Kp \geq 7$, respectively. From Figure 4a the transit times were scattered over a large range from about 30 hours to 120 hours. From the figures we found a weak correlation between the CME projected speed and the transit time. *St. Cyr et al.* [2000]

Table 1. Statistics of Frontside/Geoeffective Halo CMEs and Associated Solar Flares

	1997 ^a	1998	1999	2000	Total
Frontside halo CMEs	11	22	44	55	132
Solar flares ^b	6	13	30	44	93
Percent	55%	59%	68%	80%	70%
Geoeffective halo CMEs	7	10	13	29	59
Solar flares ^b	4	7	11	28	50
Percent	57%	70%	85%	97%	85%
Increment	2%	11%	17%	17%	15%

^aBegin at March 1997.

^bImportance greater than C.

and *Cane et al.* [2000] also derived the loose relationship despite using a different transit time. The general trend is that the larger the projected speed is, the shorter is the transit time. Nevertheless, a good correlation between transit times and CME projected speeds is shown in Figure 4b for $Kp \geq 7$ events. To illustrate the general characteristic of their relationship, we fitted these data by using a comparatively simple formula

$$T_{au} = 27.98 + \frac{2.11 \times 10^4}{V}, \quad (1)$$

where T_{au} (hour) is the transit time and V (km/s) is the projected speed of CMEs. The correlation is significant at

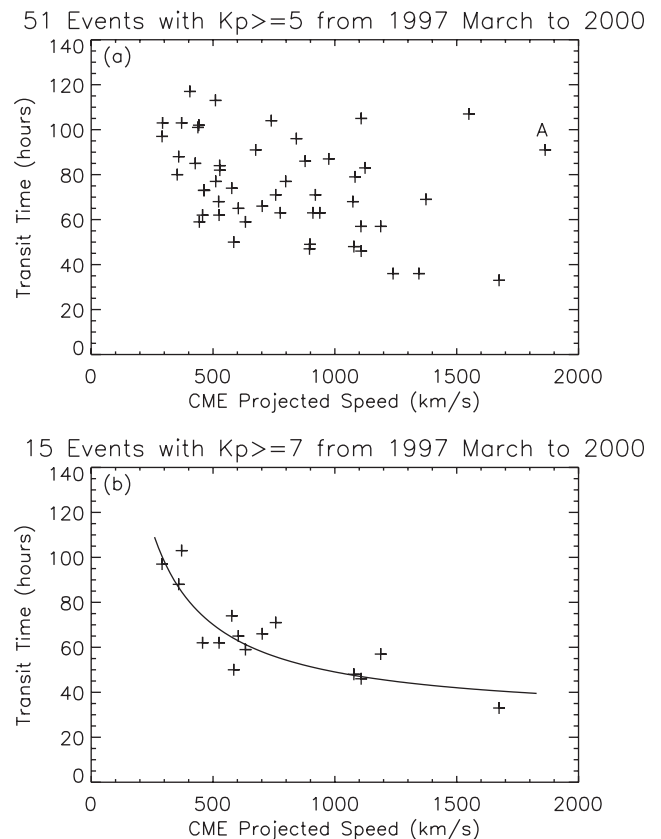


Figure 4. Transit time versus projected speed of CMEs. (a) 51 events with $Kp \geq 5$ are plotted and the transit times are scattered over a large range. (b) 15 events with $Kp \geq 7$ are plotted. The curve in Figure 4b implies a high correlation between transit time and CME projected speed with $Kp \geq 7$.

the confidence level of 99% with ~ 0.87 correlation coefficient. In any case, T_{au} must be >27.98 hours by this formula. Evidently, it was an arbitrary choice of empirical formula and the fitted curve probably was not a good representation of the data. However, we thought it was enough to just represent the general relationship between transit time and CME projected speed.

4. Summary and Discussion

[19] On the basis of the statistical study by using the LASCO, EIT, Wind, and GOES-8 observations and information about geomagnetic index Kp, we summarize and discuss the results in the following:

1. We confirm the result that only a part of frontside halo CMEs can cause moderate to severe geomagnetic storms [Cane *et al.*, 2000]. From a more complete sample we identify that only 45% of Earth-directed halo CMEs are geoeffective. Further, only 26% of Earth-directed halo CMEs can cause severe geomagnetic storms with $K_p \geq 7$.

2. Burlaga *et al.* [2001] discussed fast ejecta observed at 1 AU during 1998–1999. They found that some of the complex ejecta could have been produced by the interaction of two or more CMEs. So, one can expect the situation that one Kp storm is caused by multiple CMEs. The concept of homologous CMEs (J. X. Wang, J. Zhang, T. Wang, Y. Liu, Y. Li, and N. V. Nitta, Initiation of homologous coronal mass ejections, submitted to *Astrophysics Journal*, 2002) seems to be a good explanation for such events. In our instance, mentioned in section 2.2 last paragraph, those serial CMEs were identified as homologous CMEs by Zhang and Wang, [2002] because (1) each member of them associated with a member of homologous flare, (2) extended EUV dimming was similar, and (3) the coronagraph appearance was resembling. So, we think that those CMEs caused the Kp storm on 27 November 2000.

3. This paper uses the EUV dimming rather than the flare location as the CME initial site. The majority of initial locations of the frontside halo CMEs are around $\pm 30^\circ$ in latitude. This is reasonable because the most active regions appear in medial latitude zone. This result is also agreement with other works [e.g. Webb *et al.*, 2000; Cane *et al.*, 2000; Gopalswamy *et al.*, 2000]. However, for the CMD distribution of the geoeffective halo CMEs, our result is not consistent with theirs. Webb *et al.* [2000] suggested that the halo CMEs associated with surface activity within 0.5 Rs of Sun center appear to be an excellent indicator of increased geoactivity 3–5 days later. However, there were only six events in their work. Cane *et al.* [2000] studied 27 Earth-directed halo CMEs and pointed out that the locations of typical geoeffective solar events were in longitude $< \sim 40^\circ$ east and west. The CMEs studied by Gopalswamy *et al.* [2000] originated near the central meridian with average longitude about 17° , then only the Earth will not miss the CMEs. In our statistics the CMD distribution is asymmetrical about the center meridian. More than 60% events occurred on the west. The CMEs' initial locations scattered in latitude [S40, N40] and in longitude [E40, W70]. This suggests that a halo CME occurring on the west site of the Sun should be easier to affect the geomagnetosphere. We think the reason probably is that the CME and/or the corresponding driven shock deflects from straight direction

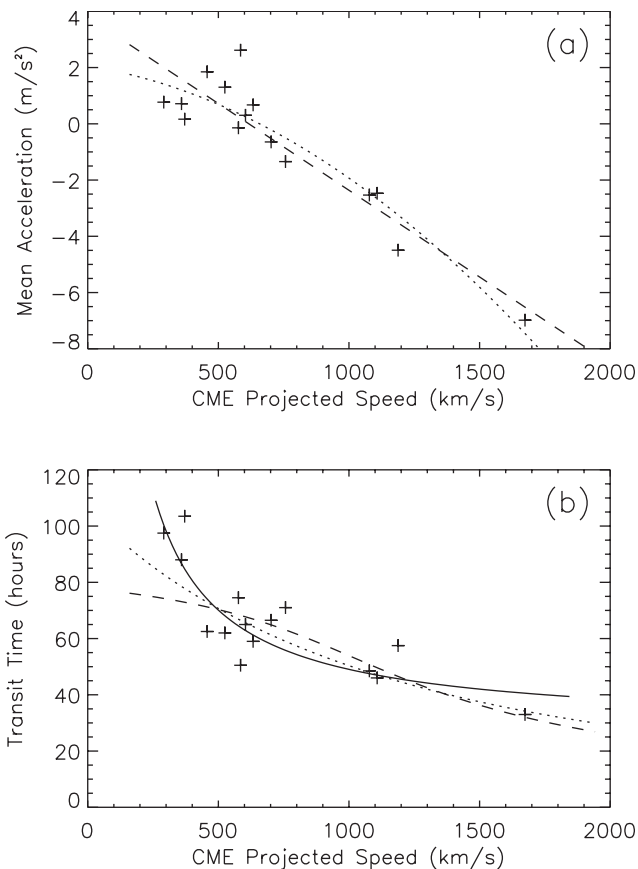


Figure 5. (a) The mean acceleration versus initial projected speed of CMEs (refer to Gopalswamy *et al.* [2001a]). The dashed line and the dotted line are the linear and quadratic fits, respectively to the data points. (b) Comparison between our fitting curve (solid one) and the prediction curves (dashed curve and dotted curve, which show the linear and quadratic acceleration cases respectively) of Gopalswamy *et al.* [2001a].

and leans to move along the Parker spiral. So, we can expect the near-west limb events to encounter the Earth rather than the near-east limb ones.

4. In the study by Brueckner *et al.* [1998] there were only 50% CMEs related to flares from March 1996 to June 1997. This is agreement with our result listed in Table 1 that 57% geoeffective halo CMEs associated with flares in 1997. Further, the percentage increased continuously with time approaching to the solar maximum. The result that 85% geoeffective halo CMEs were associated with solar flares (with importance greater than C) during the ascending phase of solar cycle 23 approves the important position of flares in aspect of space weather. As discussed in section 3.2, the increment of solar flare association from frontside ones to geoeffective ones implies that the halo CMEs associated with flares seem to have more abilities to cause geomagnetic storms.

5. Statistics represents that the average transit time of geoeffective halo CMEs is ~ 75 hours. Although the average value is primarily consistent with Brueckner *et al.* [1998] 80 hours rule, the transit times scatter in a large range (from 1 to 5 days as shown in Figure 4a). This is similar to the result obtained by Cane *et al.* [2000]. As

mentioned by Brueckner *et al.* [1998], 80 hours rule will not apply during increasing solar activity when very fast CMES are occurring. This result hints that there will probably be only one-day-ahead forecast of geomagnetic storms sometimes. Moreover, Figure 4b shows CMES of any projected speeds (from ~ 300 to 1700 km/s) are capable of producing severe geomagnetic storms. In addition, we find that a CME with a large projected speed does not always arrive the Earth in good time. For example, the point A marked in Figure 4a represents a fast (1863 km/s) but very long time (91 hours) event. The corresponding CME occurred at 1007 UT on 20 April 1998. Its source region located at S47W70 very close to the limb of solar disc. Assuming the CME's straight radial propagation, the actual Earth-directed speed of it was much smaller than the projected speed owing to the effect of projection. Meanwhile, since the CME was predominantly westward, only the eastern flank of the CME-driven shock would have arrived at 1 AU [also see Gopalswamy *et al.*, 2001b]. It is likely that it took longer to arrive at 1 AU because the flank was much weaker than the nose of the shock. Therefore the transit time between the CME appearance and the K_p maximum was prolonged unusually.

6. With restriction of $K_p \geq 7$ used, a high correlation between projected speed of geoeffective halo CMES and transit time is shown (Figure 4b). In Figure 5 we compare our empirical formula with the linear curves and quadratic curves of Gopalswamy *et al.* [2001a]. According to their method, we got the linear and quadratic fitting acceleration respectively as shown in Figure 5a and plotted the corresponding prediction curves in Figure 5b. Evidently, for the slow and fast CMES (approximately $V < 500$ km/s and $V > 1150$ km/s), the transit time from their prediction is shorter than ours. The correlation coefficient of their linear curve and quadratic curve are 0.75 and 0.83 respectively, less than that of our curve. Moreover, we calculate the mean estimated error by using the same method. The mean error of 7.5 hours for our formula is also lower than the error (10.7 hours) for their model. Although we obtain the higher correlation and decrease the average error, a fundamental difference between these two models should be noted: their model attempts to predict 1 AU arrival times of all ICMEs, but our empirical formula is only suitable for estimating the time of the severe geomagnetic storm's peak with $K_p \geq 7$. Additionally, this relationship is not good enough to predict severe geomagnetic storms since a risk of high of false alarm rate will be encountered if only the location of CME initiation and the projected speed are used in the prediction. However, at another view, if a halo CME has been suspected to cause a severe geomagnetic storm several days later, one may use this rough empirical formula for reference to forecast the arrival of K_p maximum.

[20] **Acknowledgments.** We acknowledge the use of the K_p data from WDC, the Wind spacecraft and the "LASCO CME catalog." The CME catalog is generated and maintained by the Center for Solar Physics and Space Weather, The Catholic University of America in cooperation with the Naval Research Laboratory and NASA. We also wish to acknowledge both anonymous referees for constructive comments and criticisms. This work is supported by the National Natural Science Foundation of China (49834030, 19973009) and the State Ministry of Science and Technology of China (G2000078404, 05).

[21] Shadia Rifai Habbal thanks Nat Gopalswamy and Kenneth P. Dere for their assistance in evaluating this paper.

References

- Akasofu, S.-I., Energy coupling between the solar wind and the magnetosphere, *Space Sci. Rev.*, **28**, 121, 1981.
- Arnoldy, R. L., Signature in the interplanetary medium for substorms, *J. Geophys. Res.*, **76**, 5189, 1971.
- Brueckner, G. E., J.-P. Delaboudiniere, R. A. Howard, S. E. Paswaters, O. C. St. Cyr, R. Schwenn, P. Lamy, G. M. Simnett, B. Thompson, and D. Wang, Geomagnetic storms caused by coronal mass ejections (CMEs): March 1996 through June 1997, *Geophys. Res. Lett.*, **25**, 3019, 1998.
- Burlaga, L. F., E. Sittler, F. Mariani, and R. Schwenn, Magnetic loop behind an interplanetary shock: Voyager, Helios and IMP-8 observations, *J. Geophys. Res.*, **86**, 6673, 1981.
- Burlaga, L. F., R. M. Skoug, C. W. Smith, D. F. Webb, T. H. Zurbuchen, and A. Reinard, Fast ejecta during the ascending phase of solar cycle 23: ACE observations, 1998–1999, *J. Geophys. Res.*, **106**, 20,957, 2001.
- Cane, H. V., I. G. Richardson, and O. C. St. Cyr, Coronal mass ejections, interplanetary ejecta and geomagnetic storms, *Geophys. Res. Lett.*, **27**, 3591, 2000.
- Cliver, E. W., J. Feynman, and H. B. Garrett, An estimate of the maximum speed of the solar wind, 1938–1989, *J. Geophys. Res.*, **95**, 17,103, 1990.
- Crooker, N. U., and E. W. Cliver, Postmodern view of M-regions, *J. Geophys. Res.*, **99**, 23,383, 1994.
- Crooker, N. U., and A. H. McAllister, Transients associated with recurrent storms, *J. Geophys. Res.*, **102**, 14,041, 1997.
- Gonzalez, W. D., and B. T. Tsurutani, Criteria of interplanetary parameters causing intense geomagnetic storms ($Dst < -100nT$), *Planet. Space Sci.*, **35**, 1101, 1987.
- Gopalswamy, N., A. Lara, R. P. Lepping, M. I. Kaiser, D. Berdichevsky, and O. C. St. Cyr, Interplanetary acceleration of coronal mass ejections, *Geophys. Res. Lett.*, **27**, 145, 2000.
- Gopalswamy, N., A. Lara, S. Yashiro, M. L. Kaiser, and R. A. Howard, Predicting the 1-AU arrival times of coronal mass ejections, *J. Geophys. Res.*, **106**, 29,207, 2001a.
- Gopalswamy, N., A. Lara, M. L. Kaiser, and J.-L. Bougeret, Near-Sun and near-Earth manifestations of solar eruptions, *J. Geophys. Res.*, **106**, 25,261, 2001b.
- Gosling, J. T., D. J. McComas, J. L. Phillips, and S. J. Bame, Geomagnetic activity associated with earth passage of interplanetary shock disturbances and coronal mass ejections, *J. Geophys. Res.*, **96**, 731, 1991.
- Howard, R. A., D. J. Michels, N. R. Sheeley, Jr., and M. J. Koomen, The observation of a coronal transient directed at Earth, *Astrophys. J.*, **263**, L101, 1982.
- Hudson, H. S., J. R. Lemen, O. C. St. Cyr, A. C. Sterling, and D. F. Webb, X-ray coronal changes during CMES, *Geophys. Res. Lett.*, **25**, 2481, 1998.
- Hundhausen, A. J., Sizes and locations of coronal mass ejections—SMM observations from 1980 and 1984–1989, *J. Geophys. Res.*, **98**, 13,177, 1993.
- Lindsay, G. M., J. G. Luhmann, C. T. Russell, and J. T. Gosling, Relationships between coronal mass ejection speeds from coronagraph images and interplanetary characteristics of associated interplanetary coronal mass ejections, *J. Geophys. Res.*, **104**, 12,515, 1999.
- McAllister, A. H., and N. U. Crooker, Coronal mass ejections, corotating interaction regions, and geomagnetic storms, in *Coronal Mass Ejections*, *Geophys. Monogr. Ser.*, vol. 99, edited by N. Crooker, J. A. Joselyn, and J. Feynman, pp. 279–289, AGU, Washington, D.C., 1997.
- Osherovich, V., and L. F. Burlaga, Magnetic clouds, in *Coronal Mass Ejections*, *Geophys. Monogr. Ser.*, vol. 99, edited by N. Crooker, J. A. Joselyn, and J. Feynman, pp. 157–168, AGU, Washington, D.C., 1997.
- Richardson, I. G., and H. V. Cane, Regions of abnormally low proton temperature in the solar wind (1965–1991) and their association with ejecta, *J. Geophys. Res.*, **100**, 23,397, 1995.
- Schatten, K. H., D. J. Myers, and S. Sofia, Solar activity forecast for solar cycle 23, *Geophys. Res. Lett.*, **23**, 605, 1996.
- Sheeley, N. R., R. A. Howard, M. J. Koomen, D. J. Michels, R. Schwenn, K.-H. Muhlhauser, and H. Rosenbauer, Coronal mass ejections and interplanetary shocks, *J. Geophys. Res.*, **90**, 163, 1985.
- St. Cyr, O. C., *et al.*, Properties of coronal mass ejections: SOHO LASCO observations from January 1996 to June 1998, *J. Geophys. Res.*, **105**, 18,169, 2000.
- Subramanian, P., and K. P. Dere, Source regions of coronal mass ejections, *Astrophys. J.*, **561**, 372, 2001.

- Tsurutani, B. T., W. D. Gonzalez, F. Tang, S. I. Akasofu, and E. J. Smith, Origin of interplanetary southward magnetic fields responsible for major magnetic storms near solar maximum (1978–1979), *J. Geophys. Res.*, *93*, 8519, 1988.
- Webb, D. F., E. W. Cliver, N. Gopalswamy, H. S. Hudson, and O. C. St. Cyr, The solar origin of the January 1997 coronal mass ejection, magnetic cloud, and geomagnetic storm, *Geophys. Res. Lett.*, *25*, 2469, 1998.
- Webb, D. F., E. W. Cliver, N. U. Crooker, O. C. St. Cyr, and B. J. Thompson, Relationship of halo coronal mass ejections, magnetic clouds, and magnetic storms, *J. Geophys. Res.*, *105*, 7491, 2000.
- Webb, D. F., N. U. Crooker, S. P. Plunkett, and O. C. St. Cyr, The solar sources of geoeffective structures, in *Space Weather, Geophys. Monogr. Ser.*, vol. 125, edited by S. Paul, J. S. Howard, and L. S. George, pp. 123–142, AGU, Washington, D.C., 2001.
- Zhang, J., and J. Wang, Are homologous flare-CME events triggered by moving magnetic features?, *Astrophys. J.*, *566*, L117, 2002.
-
- J. X. Wang, National Astronomical Observatories of China, Beijing 10012, China. (wjx@ourstar.bao.ac.cn)
- S. Wang and P. Z. Ye, University of Science and Technology of China, Hefei, Anhui 230026, China. (pzye@ustc.edu.cn; swan@ustc.edu.cn)
- Y. M. Wang, National Astronomical Observatories of China, Beijing, China, and University of Science and Technology of China, Jinzai Road, 96, Hefei, Anhui 230026, China. (wym@mail.ustc.edu.cn)
- G. P. Zhou, National Astronomical Observatories of China, Beijing 10012, China, and Anhui University, Hefei, Anhui, China. (zhougp@ourstar.bao.ac.cn)